Special Feature: Power Semiconductor Devices

Research Report

Effect of Carrier Lifetime and Injection Efficiency on Relationship between Forward Voltage and Reverse Recovery Charge of PiN Diode

Yusuke Yamashita and Satoru Machida

Report received on Aug. 21, 2015

ABSTRACT Silicon PiN diodes have attracted considerable attention because of their ability to be used in many applications. With the objective of reducing total power loss, the forward voltage V_f and the reverse recovery charge Q_r of silicon PiN power diodes can be controlled through two approaches based on the adjustment of either the carrier lifetime efficiency or the carrier injection efficiency. In this study, we investigate the effect of the two approaches on the relationship between V_f and Q_r for a Si PiN diode rated at 200 A/1200 V via theoretical analysis. The magnitude of V_f for a given Q_r value depends on the rate of current density decreasing dj/dt. For large values of dj/dt, carrier injection control is better suited to decrease V_f and Q_r. In contrast, for small values of dj/dt, carrier lifetime control is better suited to decrease V_f and Q_r.

KEYWORDS PiN Diode, Power Device, Carrier Lifetime, Carrier Injection, Forward Voltage, Reverse Recovery Charge

1. Introduction

With the objective of reducing the total power loss of silicon PiN power diodes, the forward voltage V_f and the reverse recovery charge Q_r of the diodes are controlled by employing one of two approaches that involve the carrier lifetime and carrier injection efficiency.[1-3]

During the on state of the PiN diode, excess carriers are injected into the i layer (intrinsic layer) from the p and n layers, and a forward voltage V_f is applied across the diode. The wattage is proportional to V_f in the on state.[4] When the diode is turned off, excess carriers are removed from the i layer, thereby producing a reverse recovery charge Q_r.[4] The turn-off loss is proportional to Q_r and the supply voltage. As the stored charge in the on state increases, V_f becomes small and Q_r becomes large; therefore, they exhibit a trade-off relationship.[4,5]

To minimize the total power loss, carrier lifetime control[2,6-10] or carrier injection efficiency control[11-18] can be used to reduce Q_r instead of increasing V_f. In previous studies, these two approaches have been investigated independently of one another. Furthermore, some studies have focused on calculating V_f and Q_r.[19-26] However, the effect of the two approaches on the V_f–Q_r trade-off curve has not thus far been investigated. Therefore, it is unclear which approach is more suitable to reduce diode power loss.

In this study, we investigate the effects of both the carrier lifetime and the carrier injection efficiency on the relationship between V_f and Q_r by theoretical analysis and analyze the suitability of both approaches in achieving power loss reduction.

2. Methods

2. 1 Outline

In this section, we describe the method of calculating V_f and Q_r for a given PiN diode. The parameters V_f and Q_r can both be calculated from the excess carrier density distribution. In this study, first, we derived a formula for the excess carrier density distribution that takes into account the effects of both the carrier lifetime and the carrier injection efficiency.

Figure 1 shows the pattern diagram of the PiN diode investigated in this study. The parameters N_p, N_i, and N_n denote the doping concentrations of the p, i, and n layers, respectively, whose respective depths are d_p, 2d, and d_n. C_i denotes the excess carrier density, J the total current density, J_{pe} the electron current density at the p/i interface caused by diffusion, J_i the recombination current density in the i layer, and J_{nh}

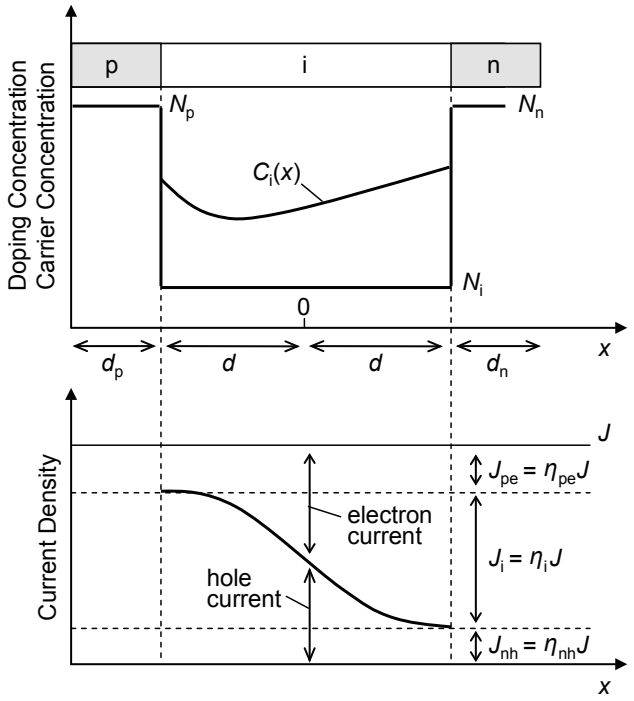

Fig. 1 Pattern diagram of PiN diode investigated in our study.

the hole current density at the i/n interface caused by diffusion. The parameters η_{pe}, η_i, and η_{nh} denote the current density ratios of J_{pe}, J_i, and J_{nh}, respectively. The hole injection efficiency γ_h of the p layer can be represented as $\gamma_h = (1 - \eta_{pe})$. Hereafter, carrier injection efficiency control is called γ_h control. The symbols and parameters used in the study are listed in **Table 1**.

In the second stage of the study, we compared the theoretically calculated values with those obtained via simulations for a Si diode with a rating of 200 A/1200 V and a total thickness of 144 μm. The other device parameters were p and n layer thicknesses of 2 μm, an i layer thickness of 140 μm, and a device area of 1 cm^2.

2. 2 Excess Carrier Density Distribution $C_i(x)$

From Fig. 1, the excess carrier density distribution $C_i(x)$ is expressed as[20,27,28]

$$C_i(x) = J\eta_i \frac{\tau_i}{2qL_{ia}} \left\{ \frac{\cosh(x/L_{ia})}{\sinh(d/L_{ia})} - B' \frac{\sinh(x/L_{ia})}{\cosh(d/L_{ia})} \right\}, \quad (1)$$

where τ_i is the carrier lifetime and L_{ia} the ambipolar length. Hereafter, carrier lifetime control is called τ_i control. The constant B' is defined as

$$B' = \frac{1}{\eta_i}(B + \eta_{nh} - \eta_{pe}), \quad (2)$$

and B is expressed as

$$B = \frac{\mu_{ie}/\mu_{ih} - 1}{\mu_{ie}/\mu_{ih} + 1}, \quad (3)$$

where μ_{ie} and μ_{ih} are the electron and hole mobility, respectively, in the i layer. The term B represents the electron and hole mobility. If $\mu_{ie} = \mu_{ih}$, B becomes zero. The term B' represents the diffusion currents and the recombination current. For $\eta_i \approx 1$, B' becomes B.

The total current density J, the electron current density J_{pe} at the p/i interface, and the hole current density J_{nh} at the i/n interface are related as[27,28]

$$J = J_{pe} + J_i + J_{nh} = J(\eta_{pe} + \eta_i + \eta_{nh}), \quad (4)$$

$$\eta_{pe} + \eta_i + \eta_{nh} = 1, \quad (5)$$

$$J_{pe} = q\frac{D_{pe}}{L_{pe}} \coth\left(\frac{d_p}{L_{pe}}\right) \frac{C_i(-d)^2}{N_p} = h_p \frac{C_i(-d)^2}{N_p}, \quad (6)$$

$$J_{nh} = q\frac{D_{nh}}{L_{nh}} \coth\left(\frac{d_n}{L_{nh}}\right) \frac{C_i(+d)^2}{N_n} = h_n \frac{C_i(+d)^2}{N_n}, \quad (7)$$

$$h_p = \frac{D_{pe}}{L_{pe}N_p} \coth\left(\frac{d_p}{L_{pe}}\right), \quad (8)$$

$$h_n = \frac{D_{nh}}{L_{nh}N_n} \coth\left(\frac{d_n}{L_{nh}}\right), \quad (9)$$

where L_{pe} and L_{nh} are the electron and hole diffusion lengths, respectively, and D_{pe} and D_{nh} are the electron and hole diffusion constants in the p and n layers, respectively.

From Eqs. (2)-(7), we obtain the following equations:

$$\eta_i = \frac{-M^2(1+B') \pm M^2\sqrt{(1+B')^2 + \dfrac{16Ah_p\mu_n(M^2+B')^2}{M^2(\mu_p+\mu_n)}}}{4Ah_p(M^2+B')^2}, \quad (10)$$

$$\eta_i = \frac{-M^2(1+B') \pm M^2\sqrt{(1+B')^2 + \dfrac{16Ah_n\mu_p(M^2-B')^2}{M^2(\mu_p+\mu_n)}}}{4Ah_n(M^2-B')^2}, \quad (11)$$

where

Table 1 Definitions of symbols and parameters used for calculation.

Symbol	Definition	Symbol	Definition
V_f	Forward voltage	η_i	Current density ratio of J_i
Q_r	Reverse recovery charge	η_{nh}	Current density ratio of J_{nh}
Q_0	Stored charge in on-state	γ_h	Carrier injection efficiency
N_p	Doping concentration of p layer	τ_i	Carrier lifetime of i layer
N_i	Doping concentration of i layer	L_{ia}	Diffusion length of i layer
N_n	Doping concentration of n layer	L_{pe}	Electron diffusion length of p layer
d_p	Depth of p layer	L_{nh}	Hole diffusion length of n layer
d	Half depth of i layer	D_{pe}	Electron diffusion constant of p layer
d_n	Depth of n layer	D_{nh}	Hole diffusion constant of n layer
C_i	Excess carrier density of i layer	μ_{ie}	Electron mobility of i layer
n_i	Intrinsic carrier density	μ_{ih}	Hole mobility of i layer
J	Total current density	t_{r1}	Interval of $t = 0$ to current zero crossing
J_{pe}	Electron current density at p/i interface	t_{r2}	Interval of current zero crossing to reaching J_r
J_i	Recombination current density at i layer	t_{r3}	Interval of current reaching J_r to becoming zero
J_{nh}	Hole current density at i/n interface	$\mathrm{d}j/\mathrm{d}t$	Rate of current density decreasing in turn-off
J_r	Peak of reverse current density in turn off	$\mathrm{d}j_r/\mathrm{d}t$	Rate of current density increasing in turn-off
B	Term of the electron and hole mobilities	k	Boltzmann constant
B'	Term of diffusion and recombination current	T	Temperature
η_{pe}	Current density ratio of J_{pe}	q	Elementary charge

$$A = \frac{J\tau_i}{4qD_{ia}}, \tag{12}$$

$$M = \frac{\cosh(d/L_{ia})}{\sinh(d/L_{ia})}. \tag{13}$$

From Eqs. (10)-(13), η_i and B' can be determined, allowing γ_h to be calculated.

Figure 2 shows the excess carrier density distributions for various values of τ_i (Fig. 2(a)) and γ_h (Fig. 2(b)). With decrease in τ_i, $C_i(x)$ decreases at around the middle of the i layer. On the other hand, with decrease in γ_h, $C_i(x)$ is reduced near the left region of the device as shown in the figure. Decreases in τ_i and γ_h affect $C_i(x)$ differently.

2. 3 Forward Voltage V_f

Assuming that μ_{in} and μ_{ip} are constant in the i layer, the forward voltage V_f for currents greater than 1 A is calculated as[20,21]

$$V_f = \frac{J}{q(\mu_{ip}+\mu_{in})}\cdot\int\frac{1}{C_i(x)}\mathrm{d}x + \frac{kT}{q}\ln\left(\frac{C_i(-d)\cdot C_i(+d)}{n_i^2}\right), \tag{14}$$

where the first and second terms on the right-hand side represent the voltage across the i layer and the junction voltage, respectively.

2. 4 Reverse Recovery Charge Q_r

Figure 3 illustrates the reverse recovery current as a function of time. t_{r1} is the interval from when the current starts decreasing to when it reaches zero, t_{r2} is the interval from when the current is zero to when it reaches the peak reverse current density J_r, and t_{r3} is the interval from when the current is J_r to when it again reaches zero. The derivative $\mathrm{d}j/\mathrm{d}t$ is the rate of current density decreasing, and $\mathrm{d}j_r/\mathrm{d}t$ is the rate at which it increases, assuming that there are no rapidly falling recovery currents (snap-offs). Q_r can be derived by defining t_{r2} and t_{r3} for a given $\mathrm{d}j/\mathrm{d}t$. During reverse

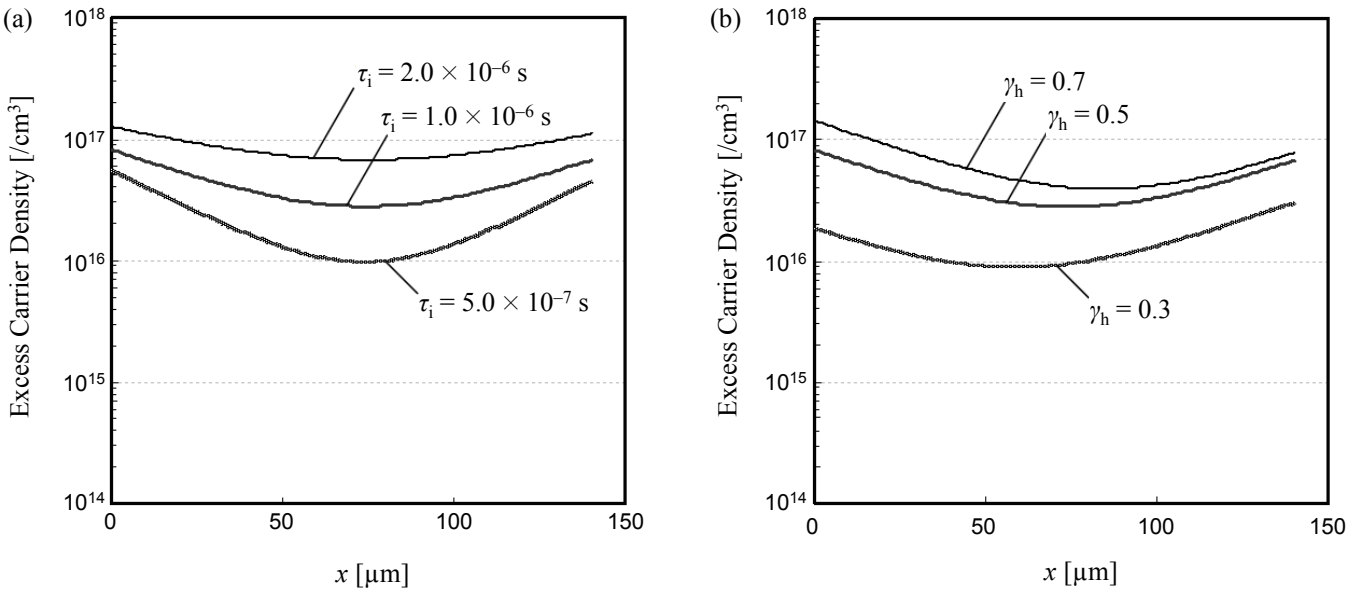

Fig. 2 Excess carrier density distributions for (a) various carrier lifetimes τ_i and (b) carrier injection efficiencies γ_h.

recovery, the number of excess carriers in the i layer decreases via the flow of reverse current and carrier recombination.[29,30] Therefore, t_{r2} and t_{r3} can be defined by calculating the time interval over which the number of excess carriers decreases to zero.

2. 4. 1 On State ($t = 0$)

The stored charge Q_0 at $t = 0$, which is the number of excess carriers at $t = 0$, can be derived as

$$Q_0 = \int_{-d}^{+d} C_i(x)\mathrm{d}x. \tag{15}$$

In this state, the decrease in charge over the interval τ_i via carrier recombination is equal to the increase in charge via J_i.

2. 4. 2 Phase 1 ($0 < t < t_1$)

During the interval defined as Phase 1 in Fig. 3, the balance of the decrease in charge (via carrier recombination) and the increase in charge (via J_i) is changed when J_i is decreased. Consequently, $Q(t)$ can be expressed as the differential equation[31]

$$\frac{\mathrm{d}Q(t)}{\mathrm{d}t} = \frac{Q(t)}{\tau_i} + \left(J_i - \frac{\mathrm{d}j}{\mathrm{d}t}\frac{J_i}{J}t\right). \tag{16}$$

The solution to Eq. (12) is given as

$$Q(t)_1 = Q_1 = \tau_i^2 \frac{\mathrm{d}j}{\mathrm{d}t}\frac{J_i}{J}(1 - e^{-t_1/\tau_i}) + \tau_i J_i(1 - e^{-t_1/\tau_i}) - \frac{\mathrm{d}j}{\mathrm{d}t}\frac{J_i}{J}\tau_i t_1 + Q_0 e^{-t_1/\tau_i}, \tag{17}$$

with the boundary condition $Q(0) = Q_0$.

2. 4. 3 Phase 2 ($t_1 < t < t_2$)

During the interval defined as Phase 2 in Fig. 3, the direction of the current reverses. This means that carriers from the p and n layers to the i layer become zero. Therefore, Q decreases via J and the carrier recombination. Thus, $Q(t)$ can be described as[31,32]

$$\frac{\mathrm{d}Q(t)}{\mathrm{d}t} = \frac{Q(t)}{\tau_i} - \frac{\mathrm{d}j}{\mathrm{d}t}t. \tag{18}$$

Eq. (14) can be solved as

$$Q(t_2) = Q_2 = \tau_i^2 \frac{\mathrm{d}j}{\mathrm{d}t}(1 - e^{-(t_2 - t_1)/\tau_i}) - \frac{\mathrm{d}j}{\mathrm{d}t}\tau_i(t_2 - t_1) + Q_1 e^{-(t_2 - t_1)/\tau_i}, \tag{19}$$

with the boundary condition $Q(t_1) = Q_1$.

2. 4. 4 Phase 3 ($t_2 < t < t_3$)

During Phase 3, $Q(t)$ can be described as

$$\frac{dQ(t)}{dt} = \frac{Q(t)}{\tau_i} - \left(J_r - \frac{dj_r}{dt}t\right). \quad (20)$$

We solve Eq. (16) as

$$Q(t_3) = \tau_i^2 \frac{dj_r}{dt}(e^{-(t_3-t_2)/\tau_i} - 1) + \tau_i\left[J_r(e^{-(t_3-t_2)/\tau_i} - 1) + \frac{dj_r}{dt}(t_3 - t_2)\right] + Q_2 e^{-(t_3-t_2)/\tau_i} = 0, \quad (21)$$

with the boundary condition $Q(t_2) = Q_2$.

2. 4. 5 Calculation

If $t_r = t_{r2} = t_{r3} = t_2 - t_1 = t_3 - t_2$, we obtain

$$Q(t_3) = \left(Q_1 - \tau_i^2 \frac{dj}{dt}\right)e^{-2t_r/\tau_i} + 2\tau_i^2 \frac{dj}{dt}e^{-t_r/\tau_i} - \tau_i^2 \frac{dj}{dt} = 0, \quad (22)$$

from Eqs. (17), (19), and (21). Here,

$$Q_1 = \tau_i^2 \frac{dj}{dt}\frac{J_i}{J}(1 - e^{-t_1/\tau_i}) + \tau_i J_i(1 - e^{-t_1/\tau_i}) - \frac{dj}{dt}\frac{J_i}{J}\tau_i t_1 + Q_0 e^{-t_1\tau_i}, \quad (23)$$

$$t_1 = J / \frac{dj}{dt}. \quad (24)$$

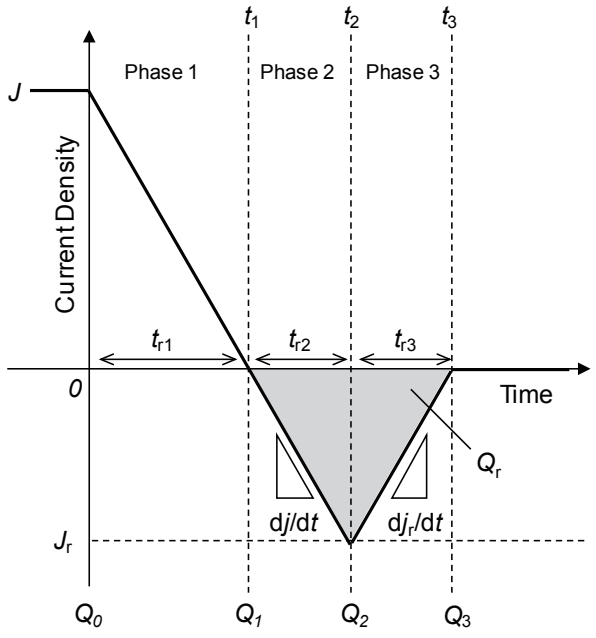

Fig. 3 Reverse recovery current as a function of time.

The solution to Eq. (22) is given as

$$t_r = \tau_i \ln\left(\frac{\sqrt{Q_1}}{\tau_i\sqrt{dj/dt}} + 1\right). \quad (25)$$

Consequently, Q_r can be calculated as

$$Q_r = \frac{dj}{dt}t_r^2. \quad (26)$$

3. Results

Figures 4(a) and (b) compar the simulated and calculated V_f–Q_r values obtained by τ_i and γ_h control, respectively. The simulation was carried out using the Sentaurus Device TCAD. Figure 4 demonstrates sufficient agreement between the simulated and calculated values for both control methods.

Figure 5 compares the V_f–Q_r values obtained by τ_i and γ_h control. For large dj/dt (Fig. 5(a)), V_f with τ_i control is greater than that with γ_h control for the same value of Q_r. Conversely, for small dj/dt (Fig. 5(b)), V_f with τ_i control is relatively small.

These results imply that the V_f–Q_r trade-off depends on dj/dt. **Figure 6** shows the dj/dt dependence of Q_r for constant V_f. In the region of small dj/dt (dj/dt < 1100 A/μs·cm^2), Q_r with τ_i control is smaller than that with γ_h control. Furthermore, in the region of large dj/dt (dj/dt > 1100 A/μs·cm^2), Q_r with γ_h control is smaller.

Therefore, at large values of dj/dt , carrier injection control is the more appropriate V_f–Q_r control method, whereas at small dj/dt values, carrier lifetime control is more appropriate.

4. Discussion

Figure 7 illustrates the relationship between the on state stored charge Q_0 and V_f with τ_i and γ_h control approaches. In the small Q_0 region, V_f with τ_i control is greater than that with γ_h control. This result implies that decreasing τ_i leads to increased device resistivity. **Figures 8** and **9** compare the distributions of the excess carrier density and the resistivity, respectively, obtained with τ_i and γ_h control approaches for a given value of Q_0. The excess carrier density distribution obtained with τ_i control exhibits a large difference between the maximum and minimum values. Therefore, τ_i control yields the highest resistivity in the middle of the i layer.

Figure 10 illustrates the relationship between Q_0 and Q_r. Q_0 is reduced via carrier recombination before the charges are swept out as the reverse current. Therefore, Q_r obtained with τ_i control is lower than that obtained with γ_h control. Furthermore, at small dj/dt values, the Q_r reduction effect increases.

Thus, the V_f–Q_r trade-off curve is defined by the effects of the phenomena demonstrated in Figs. 9 and 10. Hence, the V_f–Q_r trade-off depends on dj/dt.

5. Conclusions

The effect of the carrier lifetime and the carrier injection efficiency on the relationship between the forward voltage V_f and the reverse recovery charge Q_r of a silicon PiN diode was investigated by theoretical analysis. As the carrier lifetime decreased, V_f was observed to increase for a given stored charge Q_0. This is because the small carrier lifetime leads to the

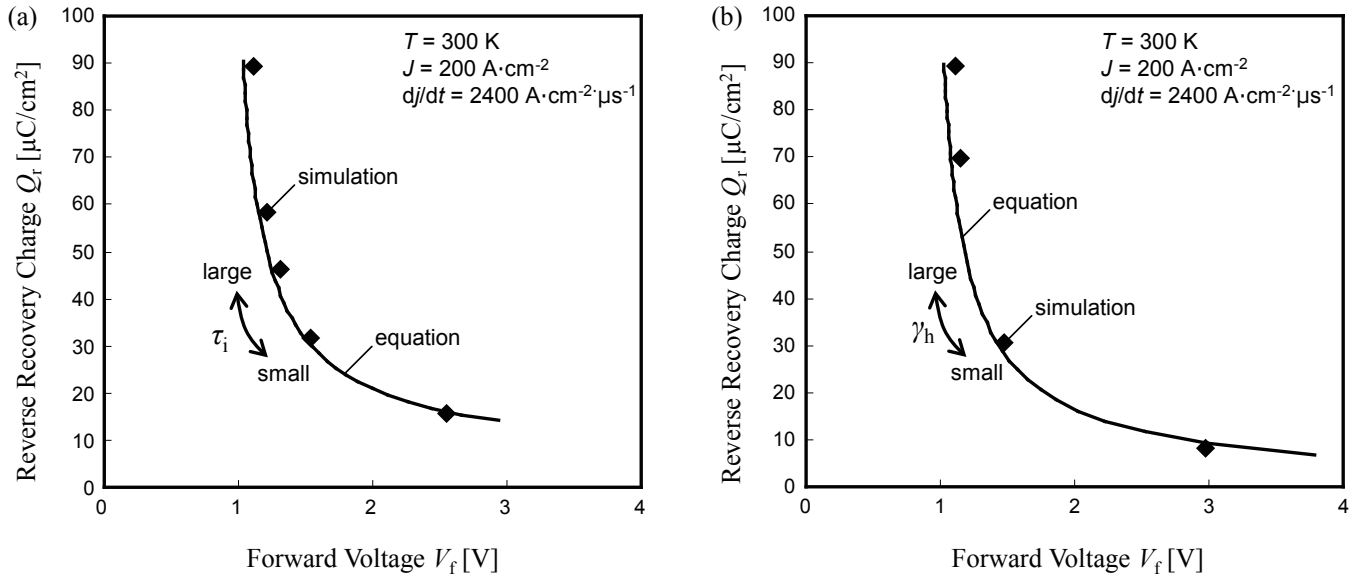

Fig. 4 Comparison between simulated V_f–Q_r data and V_f–Q_r curve calculated from Eqs. (10) and (19)-(22). (a) carrier lifetime control and (b) carrier injection control.

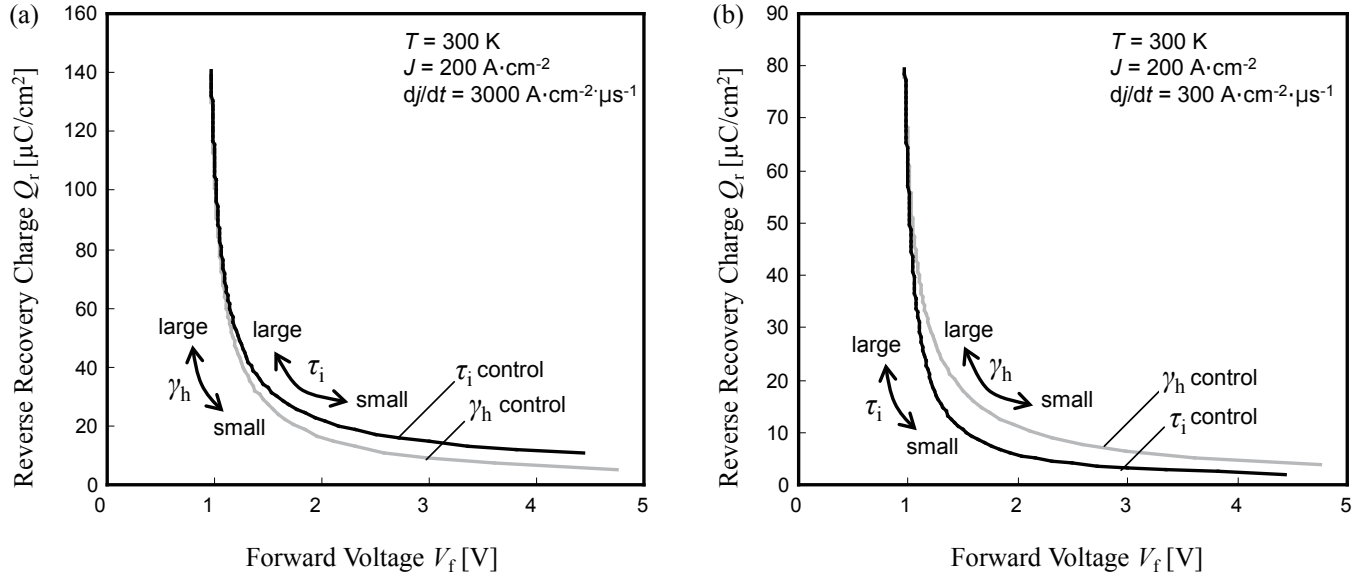

Fig. 5 Comparison of V_f–Q_r curves between carrier lifetime control and carrier injection control for (a) large values of dj/dt and (b) small values of dj/dt.

formation of a high- resistivity region in the middle of the i layer. As the carrier lifetime and dj/dt decreased, Q_r decreased via carrier recombination. The V_f–Q_r trade-off thus depends on the carrier lifetime and dj/dt. Consequently, the power loss in PiN diodes can be reduced by the appropriate carrier control method according to the dj/dt value. In the case of large dj/dt values (high frequencies), carrier injection control is more suitable to reduce power loss. For small dj/dt values, carrier lifetime control is more suitable. We believe that our results can contribute to improving the functional efficiency of PiN diodes.

6. Acknowledgements

This paper is reprinted and modified from the original publication of the Japan Society of Applied Physics by Yusuke Yamashita and Satoru Machida,

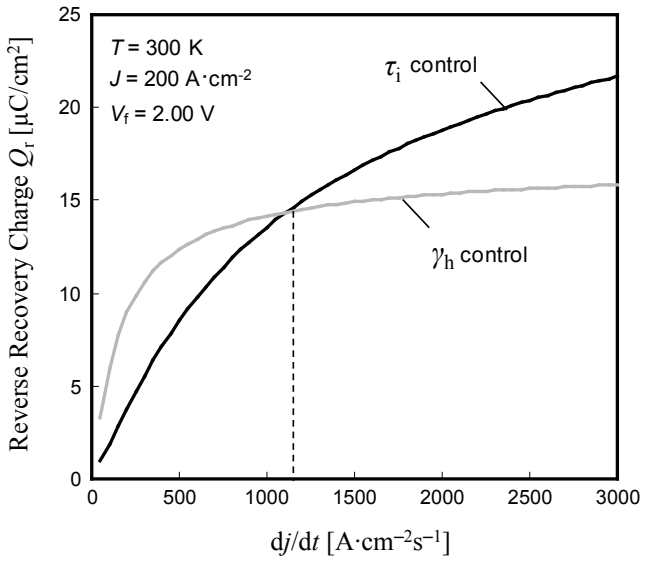

Fig. 6 dj/dt dependence of Q_r at same V_f.

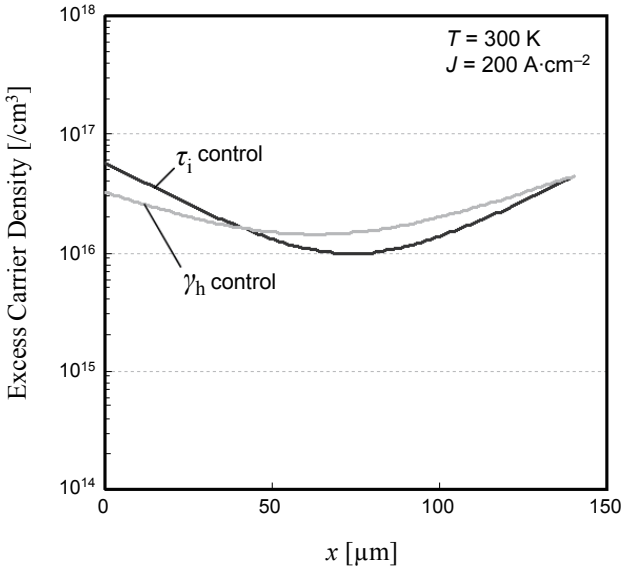

Fig. 8 Comparison of distributions of excess carrier density between carrier lifetime and carrier injection controls.

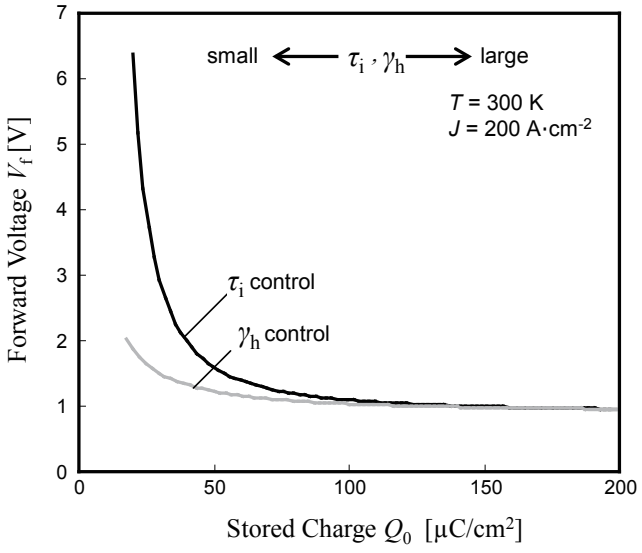

Fig. 7 Relationship between stored charge Q_0 in the on-state and forward voltage V_f.

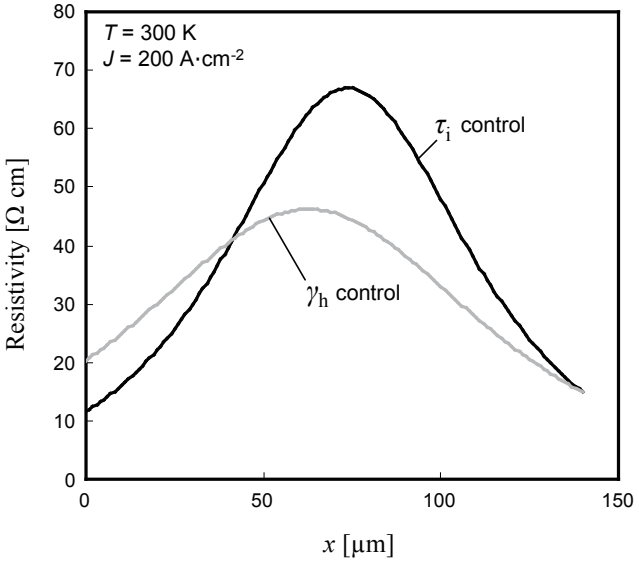

Fig. 9 Comparison of distributions of resistivity between carrier lifetime and carrier injection controls.

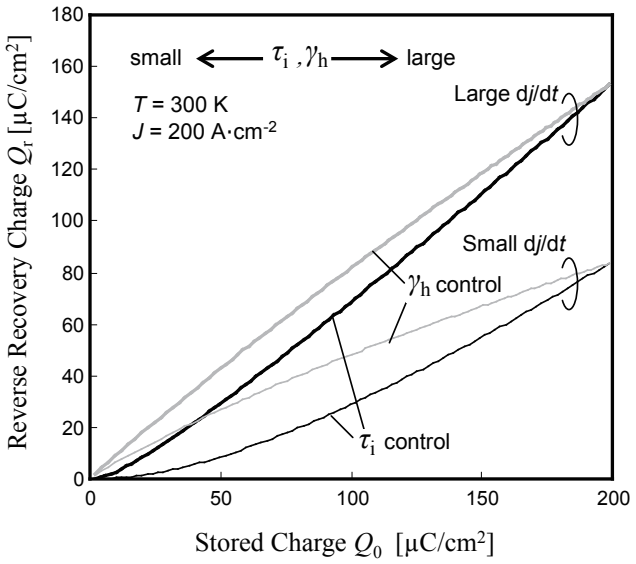

Fig. 10 Relationship between stored charge Q_0 in the on-state and reverse recovery charge Q_r.

entitled "Theoretical Analysis of Forward Voltage and Reverse Recovery Charge of Silicon p–i–n Diodes," Japanese Journal of Applied Physics, Vol. 54 (2015), 04DP01(http://dx.doi.org/10.7567/JJAP.54.04DP01), ©2015 JSAP, with permission from the Japan Society of Applied Physics.

References

(1) Nemoto, M. et al., *Proc. Int. Symp. Power Semiconductor Devices and ICs* (2000), p. 119, IEEE.
(2) Vobecký, J. and Hazdra, P., *IEEE Electron Device Lett*., Vol. 26 (2005), p. 873.
(3) Baliga, B. J. and Sun, E., *IEEE Trans. Electron Device*, Vol. 24 (1977), p. 685.
(4) Baliga, B. J., *Power Semiconductor Devices* (1995), p. 153, PWS Publishing Company.
(5) Lutz, J. et al., *Semiconductor Power Devices* (2011), p. 184, Springer.
(6) Vobecký, J. and Hazdra, P., *Nucl. Instrum. Methods Phys. Res. Sect. B*, Vol. 253 (2006), p. 162.
(7) Hazdra, P. and Komarnitsky, V., *Microelectron. J*., Vol. 37 (2006) , p. 197.
(8) Nemoto, M. et al., *Proc. Int. Symp. Power Semiconductor Devices and ICs* (2004), p. 433, IEEE.
(9) Hazdra, P. et al., *Microelectron. J*.,Vol. 35 (2004), p. 249.
(10) Onozawa, Y. et al., *Proc. Int. Symp. Power Semiconductor Devices and ICs* (2008), p. 80, IEEE.
(11) Porst, A. et al., *Proc. Int. Symp. Power Semiconductor Devices and IC* (1997), p. 213, IEEE.
(12) Hille, F. et al., *Proc. Int. Symp. Power Semiconductor Devices and ICs* (2007), p. 109, IEEE.
(13) Chen, M. et al., *Proc. Int. Symp. Power Semiconductor Devices and ICs* (2006), p. 9, IEEE.
(14) Pfaffenlehner, M. et al., *Proc. Int. Symp. Power Semiconductor Devices and ICs* (2011), p. 108, IEEE.
(15) Baliga, B. J., *IEEE Electron Device Lett*., Vol. 8 (1987), p. 407.
(16) Cappelluti, F. et al., *Microelectron. J*., Vol. 37 (2006), p. 190.
(17) Tornblad, O. et al., *Proc. Int. Symp. Power Semiconductor Devices and ICs* (1995), p. 380, IEEE.
(18) Schlangenotto, H. et al., *IEEE Electron Device Lett*., Vol. 10 (1989), p. 322.
(19) Omura, I. et al., *Proc. Int. Workshop Physics of Semiconductor Devices* (2007), p. 781, IEEE.
(20) Baliga, B. J., *Power Semiconductor Devices* (1995), p. 155, PWS Publishing Company.
(21) Lutz, J., *Semiconductor Power Devices* (2011) p. 167, Springer.
(22) Naito, M. et al., *IEEE Trans. Electron Devices*, Vol. 23 (1976), p. 945.
(23) Vobecký, J. et al., *Solid-State Electron*., Vol. 47 (2003), p. 45.
(24) Vobecký, J. et al., *Microelectron. J*., Vol. 43 (2003), p. 537.
(25) Vobecký, J. et al., *Microelectron. J*., Vol. 40 (2000), p. 427.
(26) Anand, R. S. et al., *Solid-state Electron*., Vol. 47 (2003), p. 83.
(27) Herlet, A., *Solid-state Electron*., Vol. 11 (1968), p. 717.
(28) Perpina, X. et al., *J. Electrochem. Soc*., Vol. 157 (2010), p. 711.
(29) Benda, H. and Spenke, E., *Proc. IEEE*, Vol. 55 (1967), p. 1331, IEEE.
(30) Baburske, R. et al., *IEEE Trans. Electron Devices*, Vol. 55 (2008), p. 2164.
(31) Baliga, B. J., *Power Semiconductor Devices* (1995), p. 171, PWS Publishing Company.
(32) Rahimo, M. T. and Shammas, N. Y. A., *IEEE Trans. Ind. Appl*., Vol. 37 (2001), p. 661.

Figs. 1, 2(a), 3-5, 7 and 10
Reprinted from Proc. Workshop of IEEJ , Vol. EDD-14, No. 66-80 (2014), pp. 69-73, Yamashita, Y. and Machida, S., Effect of Carrier Lifetime and Injection Efficiency to Relationship Between Forward Voltage and Reverse Recovery Charge of Pin Diode, © 2014 IEEJ, with permission from the Institute of Electrical Engineers of Japan

Figs. 2(b), 8-9 and Table 1
Reprinted from Japanese Journal of Applied Physics, Vol. 54 (2015), 04DP01, Yamashita, Y. and Machida, S., Theoretical Analysis of Forward Voltage and Reverse Recovery Charge of Silicon p–i–n Diodes, ©2015 JSAP, with permission from the Japan Society of Applied Physics.

Yusuke Yamashita
Research Field:
- Power Semiconductor Devices

Academic Society:
- The Japan Society of Applied Physics

Award:
- Technical Committee Encouragement Award on IEEJ Transactions on Electronics, Information and Systems, 2015

Satoru Machida
Research Field:
- Power Semiconductor Devices

Academic Degree: Dr.Eng.
Academic Society:
- The Institute of Electrical Engineers of Japan

